Miloslav KOSEK, Martin TRUHLAR, Ales RICHTER

Technical university of Liberec

Skin effect in massive conductors at technical frequencies

Abstract. *Current distribution in massive conductor of rectangular cross section due to the skin effect is given by a simple formula. Unusual features follow from the formula, therefore experimental verification is necessary. Since the current density cannot be measured, magnetic field of the conductor is calculated by the combination of analytical formula and numeric integration. Then, the high precision measurement of magnetic field can be used in order to verify the current density distribution and its interpretation. The second use of results is the calculation of forces between conductors with high currents. Theory leading to analytical formulae and important numerical results are presented in the paper.*

Streszczenie. *Efekt naskórkowości w litym przewodzie o przekroju prostokątnym jest opisany prostymi zależnościami, ale konsekwencje tych zależności są na tyle niezwykłe, że wymagają weryfikacji eksperymentalnej. Ponieważ nie da się mierzyć gęstości prądu, wykorzystano do weryfikacji indukowane pole magnetyczne, które obliczono przez połączenie wzorów analitycznych i metod numerycznych. Otrzymane wyniki porównano z dokładnymi pomiarami pola magnetycznego, co pozwala zweryfikować faktyczny rozkład gęstości prądu. Wyniki obliczeń można też wykorzystać do wyznaczania sił działających na przewody przy przepływie wielkich prądów. W pracy przedstawiono wyprowadzenie modelu matematycznego i najważniejsze wyniki obliczeń numerycznych.* ***(Efekt naskórkowości w litych przewodach przy niskich częstotliwościach)***

Keywords: Skin-effect, magnetic field, massive conductor, 2D current distribution, complex symbolic method
Słowa kluczowe: Efekt naskórkowości, pole magnetyczne, lite przewody, dwuwymiarowy rozkład pola, zespolona metoda symboliczna

Introduction

Strong currents flowing in distribution points can lead to high forces between conductors. In order to estimate the forces, magnetic field produced by the conductors must be known. It can be calculated from currents in conductors.

Because of high currents, distribution points use conductors of large cross section. Due to the skin effect, the current density is not uniform in them even at low technical frequencies. In this simple case the current distribution in analytical form can be derived and calculated simply. Unfortunately, the solution is in unusual complex symbolic form. Its understanding is more difficult and its improper use can lead to serious errors. Therefore, the experimental verification of results is necessary.

Since the current density cannot be measured, it should be verified from effects that are produced by it. The most important of them is the excitation of external magnetic field. It is the second, theoretical, reason why the magnetic field of used conductors should be known in detail and with a high accuracy.

Theory

Theory of the two dimensional (2D) skin effect follows from the theory of 1D skin effect [2]. Let us suppose the simplest case. The harmonic electric field propagates in the infinite conducting layer in the direction of Z axis that lies in its plane of symmetry, see Fig. 1. Then the field strength in the conducting infinite layer and in the direction normal to its surface, which is the X axis, is given by the equation

$$\frac{\partial^2 \hat{E}_z}{\partial x^2} - \mathrm{j}\omega\mu\gamma\hat{\mathrm{E}}_\mathrm{z} = 0, \tag{1}$$

where $\hat{E}_z$ is the component of electric field, $\omega = 2\pi f$ is the angular frequency (f is frequency), material parameter μ is the medium permeability and γ is its conductivity. We use complex symbolic calculus because of its simplicity and effectiveness. Then j is the imaginary unit with definition $\mathrm{j}^2 = -1$. Complex quantities are denoted by a hat sign over the symbol, e.g. $\hat{E}$.

The solution of equation (1) is searched in the form

$$\hat{E}_z(x) = \hat{A}\,\mathrm{e}^{\hat{\delta}x} + \hat{B}\,\mathrm{e}^{-\hat{\delta}x}, \tag{2}$$

where $\hat{\delta}$ is (in general complex) coefficient of attenuation and $\hat{A}$ and $\hat{B}$ are in general complex constants. By substitution of the general solution (2) into eqution (1) we find the formula for the coefficient $\hat{\delta}$.

$$\hat{\delta} = (1+\mathrm{j})\sqrt{\frac{\omega\mu\gamma}{2}}, \tag{3}$$

The constants $\hat{A}$ and $\hat{B}$ can be found from boundary conditions. In the considered case of finite layer these conditions have a form (see Fig. 1)

$$\hat{E}_z(x) = E_o \quad \text{for} \quad x = a \quad \text{and} \quad x = -a, \tag{4}$$

where E_o is the electric field strength on the layer surface. We apply the boundary conditions (4) to the general solution (2), we obtain well-known solution presented in each literature [2], for instance.

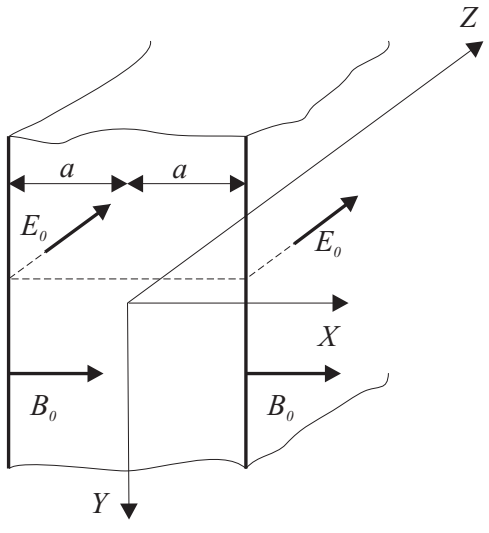

Fig. 1. Boundary conditions of 1D skineffect

The 2D skineffect is given by equation

$$\frac{\partial^2 \hat{E}}{\partial x^2} + \frac{\partial^2 \hat{E}}{\partial y^2} - \mathrm{j}\omega\mu\gamma\hat{\mathrm{E}} = 0, \tag{5}$$

where $\hat{E}(x,y)$ is the component of electric field strength. This equation has two 1D solutions in the direction of X axis and also of Y axis.

These 1D solutions have the form

$$\begin{aligned}\hat{E}_x(x) &= \hat{E}\,\mathrm{e}^{\hat{\delta}x} + \hat{F}\,\mathrm{e}^{-\hat{\delta}x},\\ \hat{E}_y(y) &= \hat{G}\,\mathrm{e}^{\hat{\delta}y} + \hat{H}\,\mathrm{e}^{-\hat{\delta}y}.\end{aligned} \tag{6}$$

The indices used at variables $\hat{E}_x$ and $\hat{E}_y$ does not mean field components. They denotes coordinate along which the electric field varies. The electric field has only the z-component.

Irrespective of the fact that these two formulae are solutions of 2D equation, they are not the most general ones. The most general solution of (5) is the product of 1D solutions (6),

$$\begin{aligned}\hat{E}_{xy}(x,y) &= \hat{E}_x(x)\hat{E}_y(y) =\\ &(\hat{a}\,\mathrm{e}^{\hat{\delta}x} + \hat{b}\,\mathrm{e}^{-\hat{\delta}x})(\hat{c}\,\mathrm{e}^{\hat{\delta}y} + \hat{d}\,\mathrm{e}^{-\hat{\delta}y}).\end{aligned} \tag{7}$$

The general solution (7) can be proved by its substitution into differential equation (5). In the formula (7) other constants are used then in formula (6), since it is another solution. After multiplication, the product (7) has the form

$$\begin{aligned}\hat{E}_{xy}(x,y) &= \hat{E}_x(x)\hat{E}_y(y) = \hat{A}\,\mathrm{e}^{\hat{\delta}(x+y)} +\\ &+\hat{B}\,\mathrm{e}^{\hat{\delta}(x-y)} + \hat{C}\,\mathrm{e}^{-\hat{\delta}(x-y)} + \hat{D}\,\mathrm{e}^{-\hat{\delta}(x+y)}.\end{aligned} \tag{8}$$

New constants $\hat{A}, \hat{B}, \hat{C}, \hat{D}$ follow from old ones $\hat{a}, \hat{b}, \hat{c}, \hat{d}$. Transformation between these two sets of coefficients is not important in this case.

We obtain general solution of equation (5) as the sum of solutions (8) and (6)

$$\begin{aligned}\hat{E}(x,y) &= \hat{A}\,\mathrm{e}^{\hat{\delta}(x+y)} + \hat{B}\,\mathrm{e}^{\hat{\delta}(x-y)} + \hat{C}\,\mathrm{e}^{-\hat{\delta}(x-y)} +\\ &+\hat{D}\,\mathrm{e}^{-\hat{\delta}(x+y)} + \hat{E}\,\mathrm{e}^{\hat{\delta}x} + \hat{F}\,\mathrm{e}^{-\hat{\delta}x} + \hat{G}\,\mathrm{e}^{\hat{\delta}y} + \hat{H}\,\mathrm{e}^{-\hat{\delta}y}.\end{aligned} \tag{9}$$

Constants should be determined from boundary conditions that require the electric field strength to have constant value E_o on the surfaces of rectangular conductor of width $2a$ in the direction of X axis and height $2b$ in the direction of Y axis, see Fig. 2. The attempt for explanation of this choice of boundary condition is in the part Discussion.

The wave propagates in the direction of Z axis. Boundary conditions have the form

$$\begin{aligned}\hat{E}(x,y) &= E_o \quad \text{for} \quad x = a,\ \ y \in (-b, b),\\ \hat{E}(x,y) &= E_o \quad \text{for} \quad x = -a,\ \ y \in (-b, b),\\ \hat{E}(x,y) &= E_o \quad \text{for} \quad y = b,\ \ x \in (-a, a),\\ \hat{E}(x,y) &= E_o \quad \text{for} \quad y = -b,\ \ x \in (-a, a).\end{aligned} \tag{10}$$

Main problem in the determinantion of unknown coefficients $\hat{A}$ through $\hat{H}$ in (9) is the fact that there are 8 unknown coefficients but only 4 boundary conditions (10). It means that some coefficients must equal one another. After some non trivial manipulation that cannot be presented here, we get the resulting electric field inside the conductor

$$\begin{aligned}\hat{E}(x,y) &= -E_o \frac{\cosh(\hat{\delta}x)\cosh(\hat{\delta}y)}{\cosh(\hat{\delta}a)\cosh(\hat{\delta}b)} +\\ &+E_o \frac{\cosh(\hat{\delta}x)}{2\cosh(\hat{\delta}a)} + E_o \frac{\cosh(\hat{\delta}y)}{2\cosh(\hat{\delta}b)}.\end{aligned} \tag{11}$$

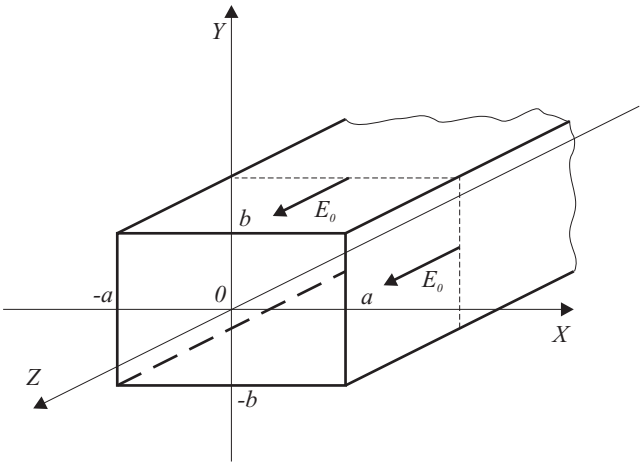

Fig. 2. Boundary conditions for 2D skin effect

By substitution $x = \pm a$ or $y = \pm b$ into (11) we find that bounadry conditions (10) are valid.

Differential Ohm's Law

$$\hat{\vec{i}} = \gamma \hat{\vec{E}}, \tag{12}$$

where $\hat{\vec{i}}$ is current density and γ is the conductivity, allows the calculation of current density, which is a well-known property. It is also a reason why the skineffect is formulated for current density in textbooks.

The magnetic field flux density can be derived at least by 4 means:

1. Differential equation,
2. Amper's Law,
3. Faraday's Law of electromagnetic induction,
4. Biot-Savart Law.

As we will see later, only the last approach makes the calculation of magnetic field outside the conductor possible.

The symbolic differential equation for magnetic field flux density $\hat{B}$ is analogical to the one (5) for electric field

$$\frac{\partial^2 \hat{B}}{\partial x^2} + \frac{\partial^2 \hat{B}}{\partial y^2} - \mathrm{j}\omega\mu\gamma\hat{\mathrm{B}} = 0, \tag{13}$$

where $\hat{B}(x,y)$ is the selected component of magnetic field flux density. Its solution can be treated quite analogically as in the previous case. But the problem is how to determine constant flux density B_o on the conductor surface, if the value of electric field strength E_o is known.

As the second possibility, Ampere's Law in differential form, we get the equation

$$\mathrm{rot}\,\hat{\vec{B}} = \mu\gamma\hat{\vec{E}}. \tag{14}$$

Since eletric field strength $\hat{\vec{E}}$ is known, we can get the magnetic flux density $\hat{\vec{B}}$ by its integration.

The third possibility uses Faraday's Law. Using the symbolic complex calculus we can derive the equation

$$\hat{\vec{B}} = -\frac{\mathrm{j}}{\omega}\,\mathrm{rot}\,\hat{\vec{E}}. \tag{15}$$

In this case we get the magnetic flux density $\hat{\vec{B}}$ by derivation of field strength $\hat{\vec{E}}$.

These three equivalent approaches calculate the magnetic flux density inside the conductor. The most complicated is the first equation (13) and the simplest is the last possibility (15).

Since the magnetic field in the conductor cannot be measured, we need another approach. The magnetic field outside the conductor can be calculated by the use of Biot-Savart Law. As we work with straight conductor, the analytical formula can be derived that speeds the calculations significantly. We neglect details here and write the formula that is valid for a very thin straight conductor in the direction of axis Z that intersect the XY plane at the point with coordinated (x_d, y_d)

$$B_x(x,y,z) = -\frac{\mu_0}{4\pi} I \frac{y-y_d}{(y-y_d)^2+(x-x_d)^2} \left[\frac{z-L}{\sqrt{(z-L)^2+K_{xy}}} - \frac{z+L}{\sqrt{(z+L)^2+K_{xy}}} \right],$$

$$B_y(x,y,z) = \frac{\mu_0}{4\pi} I \frac{x-x_d}{(y-y_d)^2+(x-x_d)^2} \left[\frac{z-L}{\sqrt{(z-L)^2+K_{xy}}} - \frac{z+L}{\sqrt{(z+L)^2+K_{xy}}} \right], \tag{16}$$

$$B_z(x,y,z) = 0,$$

where the constant K_{xy} is defined by formula

$$K_{xy} = (x-x_d)^2 + (y-y_d)^2. \tag{17}$$

In formula (16) we further suppose that the conductor has the length of $2L$ and it is positioned symmetrically with respect to the plane XY. The current I flows in the positive sense of the Z axis.

By the use of the superposition principle the magnetic field of massive straight conductor can be calculated if we divide it into a large number of thin conductors. These partial conductors have the same cross section but different coordinates (x_d, y_d). The resulting field is the sum of flux densities (16). Therefore, the magnetic field calculation can be made very simply and fast in the case of conductor of rectangular cross section.

In order to complete solution, the electric field strength outside the conductor should be determined. It can be very simply by the use of Ampere's Law (14)

$$\hat{\vec{E}} = \frac{1}{\mu\gamma} \operatorname{rot} \hat{\vec{B}}. \tag{18}$$

Unfortunately, the rotation operation should be made numerically in this case, which leads to serious numerical errors due to the derivation. From the practical point of view the another operation should be preferred using the Faraday's Law

$$\operatorname{rot} \hat{\vec{E}} = \mathrm{j}\omega \hat{\vec{B}}. \tag{19}$$

The electric field strength can be obtained form these set of equaitons by integration.

Experiment

We prepared simple distribution point in the form of three phase star connected straight conductors of rectangular cross-section. The photograph of apparatus is in Fig. 3. The width is $2a$ = 10 mm in the X axis direction and the height $2b$ = 40 mm along the Y axis. The length along the Z axis is $2d$ = 2 m. The harmonic current in conductors of approximately of 1 kA that flows along the positive Z axis is get from the secondary parts of three transformers. Their primary windings are connected to the commercial instrument Chroma 61705 that makes possible to change all the parameters of three phase system (waveform, frequency, phase voltage, phase constants, etc).

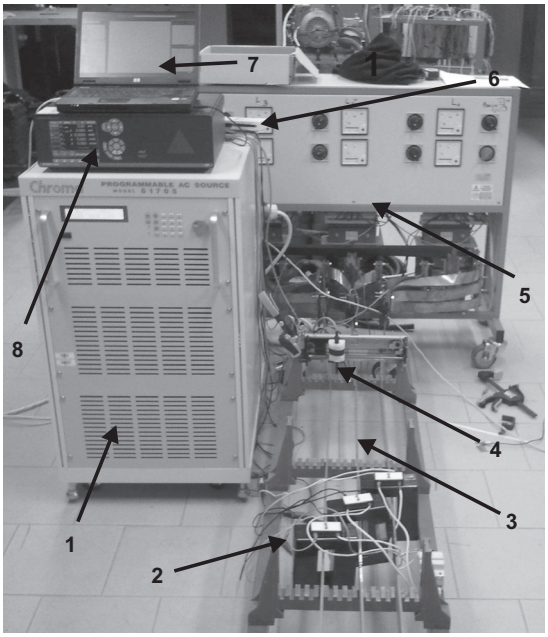

Fig. 3. Apparatus for automated measurement : 1 - Programmable AC Source 61705, 2 - Current measuring, 3 - Conductors, 4 - Linear shift with 3D Hall probe, 5 - Transformers, 6 - Sampling unit NiDaq, 7 - PC with MATLAB interface, 8 - Analyzer NORMA 5000.

The system is controlled by a computer; therefore the measurement is fully automated. Dynamical measurements in time domain were realized first. By the use of the standard analog-to-digital convertor the measured values are saved in the digital form in the computer memory. The sampling frequency can reach up 341,33 kHz and the sample length of 12 bits is sufficient for technical accuracy. Since the maximum apparatus frequency is 1200 Hz, a satisfactory number of samples are acquired for each period at each frequency. The apparatus control was programmed in the MATLAB system.

In the time domain three phase current and voltage drops on conductors are measured and recorded in the MATLAB file with the mat extension. While the currents are high, about 1000 A, the voltages are relatively low, less than 1 V. The output MATLAB file is further processed. By the use of the Fast Fourier Transform (FFT) we have found that all outputs are harmonic with high accuracy. The impedance for each conductor was calculated. Its absolute value is get from currents and the phase shift from time delay between voltage and current. While its absolute value agrees well with simple equivalent circuit in the whole frequency range, in the phase shift there are differences at high frequencies. They can be explained by the fact that conductors influence one another especially at high frequencies.

As for accompanying magnetic field measurement we have a computer controlled automated 1D movement system for the 3D Hall probe [1]. Therefore, we can measure all the components of flux density in the line. Since all the parts of apparatus are computer controlled, all the measured values are stored in the memory. For each measured point there

are 1 coordinate, three components of magnetic flux density, three phase currents and three conductor voltages. All the values are in dynamic form, over several periods with sufficient sampling rate for each measured point. The extent of numeric data is therefore large.

In the skin effect measurement only one conductor should be exited. It does not bring any problem and the experiment will be made after the full system verification.

Numerical calculations

The used coordinate system is described in the part Experiment. Current distribution was calculated simply from the equation (11). The use of formulae (16) for the calculations of all components of magnetic flux density needs the numeric integration along the conductor cross section. The cross section contains rectangular grid and the total magnetic field is a superposition from each element in the grid that is considered as a very thin conductor. The grid finest was estimated from results. Especially, in order to get the correct phase results, the grid should contain more than 10 000 elements.

In principle the problem is three dimensional. Therefore, the presentation of results is difficult. Basic possibilities are 3D graphs, flux lines, flux vectors and standard parametric graphs. Since we need exact comparison, we limited to the last possibility - parametric graphs.

In general, all the results are in complex form. We can consider either the real and imaginary part or the amplitude and phase angle. While the first possibility is suitable for the dynamic presentation, if the components are multiplied by the harmonically varying values in time, the use of the second approach, amplitude and phase, is typical for circuit theory and has a straightforward physical meaning. Therefore, we use the amplitude and phase approach whenever it is suitable.

Results for Current Density

In order to minimize the second order effect, due to the other parts of circuit, all the results are for XY plane that lies in the conductor centre. The geometry is sketched in Fig. 4.Dimensions along the Y axis are 5 times higher in experiment.

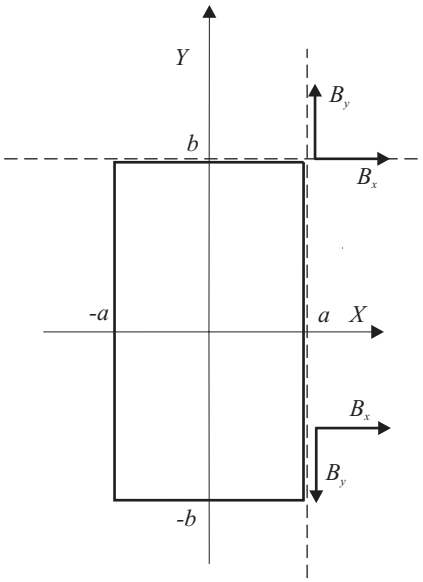

Fig. 4. Geometry used in calculations and graphs

As an example, the real component of current density calculated by formula (11) and (12) along the coordinate axis Y for different frequencies is presented in Fig. 5. In the calculations the total current I was assumed to be constant. Concentration of flowing current near conductor edges is therefore evident for higher frequencies. Opposite to the 1D case [3], the maximum of current density for lower frequencies is not at the conductor surface, but near to it.

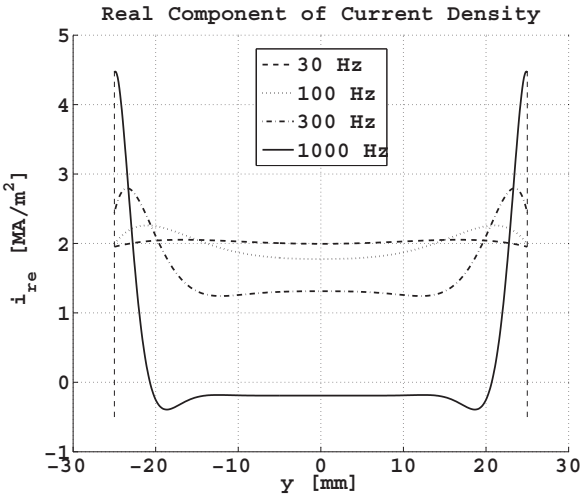

Fig. 5. Real component of current density along Y axis for several frequencies. Total current is constant and equal to 1 kA.

However, more surprising is the fact that in the central part of the conductor the current can flow in opposite direction for the case of high frequency. It is confirmed by the current density phase shift, which is in Fig. 7. At the highest frequency the phase shift is above 90° in the central part of conductor. From the circuit theory it means that this part is a source instead of load. Physically, according the differential Ohm's Law (12), it means that in this part of conductor there is a negative local conductivity.

The imaginary part of current density is in Fig. 6. The values are negative in a large inner part of the conductor. In this case the imaginary part is not a phase shift of real component by phase constant of 90°, which is typical for the 1D layer [3].

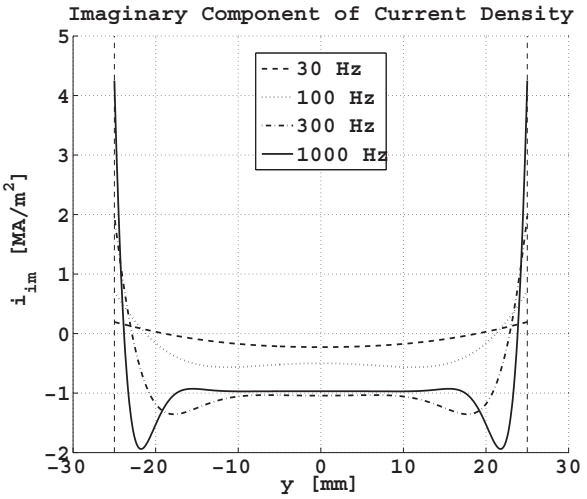

Fig. 6. Imaginary component of current density along Y axis.

Since the amplitude of current density does not differ significantly from its real component, it is not presented here. The phase shift is in Fig. 7. For high frequency it exceeds 90°.

Results for Magnetic Field

The frequency dependence of current distribution and its specific features should reflect in the magnetic field dis-

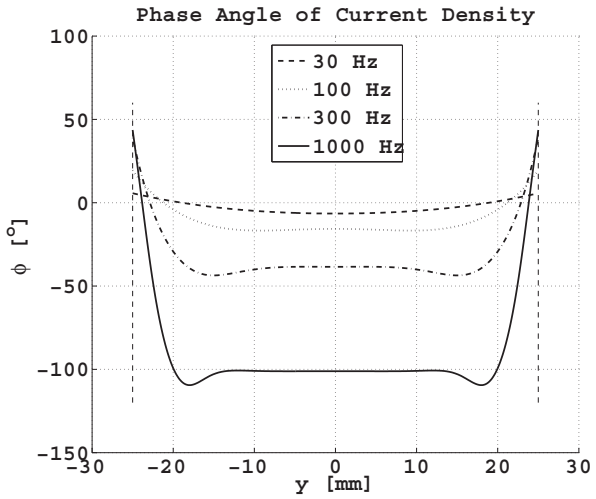

Fig. 7. Phase shift of current density along Y axis.

tribution. Both the absolute components and phase shift of magnetic flux density are presented in next figures. The amplitude can be measured directly by the Hall probe sensor, while the phase shift is defined as the shift between total exciting current and flux density components. It needs a time output from the Hall probe.

Both the variables should be measured in directions parallel to the width and the height of the conductor and very close to its surface. The corresponding lines are shown in Fig. 4 as dashed ones. Both the x and y component of flux density are shown systematically on next figures.

Amplitude and phase shift of the B_x component in the line parallel to the X axis and very close to the wire top surface, see Fig. 4, are presented in Fig. 8. The frequency effect is small, about 2 mT in amplitude and maximum 8° in phase.

Amplitude and phase of another component, B_y, for the same case are in Fig. 9. The frequency change of the amplitude is only slightly higher (3 mT) in comparison with previous case, but the change of phase constant is more then 20°.

The frequency dependence of flux density along the wider side of the wire at its left hand side and very close to it is in next figures. The flux density is calculated on the line parallel to the Y axis, see the dashed vertical line in Fig. 4. The amplitude and phase for the x-component are in Fig. 10. As for amplitude, there is no systematic behavior; maximum change of typical value of 3 mT is at wire edge. The phase change is systematic in most of the considered range and in the wire centre it achieves a high value of almost 30°.

The frequency effect on the y-component at the same conditions is in Fig. 11. Again there is no system in amplitude dependence, its maximum change at the wire edge has a typical value of about 3 mT. The phase change is almost systematic and its maximum value is about 15°.

Since the effect of frequency on the phase shift is higher in all the cases, we present in Fig. 12 the frequency dependence of the phase shift for several positions, as a parameter, on the upper horizontal surface of the wire, see Fig. 4. Therefore, the parameter is the x-coordinate of the probe. At the frequencies above about 100 Hz the phase shift depends on the probe position significantly and the highest value is at the wire edge. For the case of vertical surface the phase shift is even higher.

For completeness the vector form of magnetic flux density is in Fig. 13. The highest values are on the top and bottom part of the conductor.

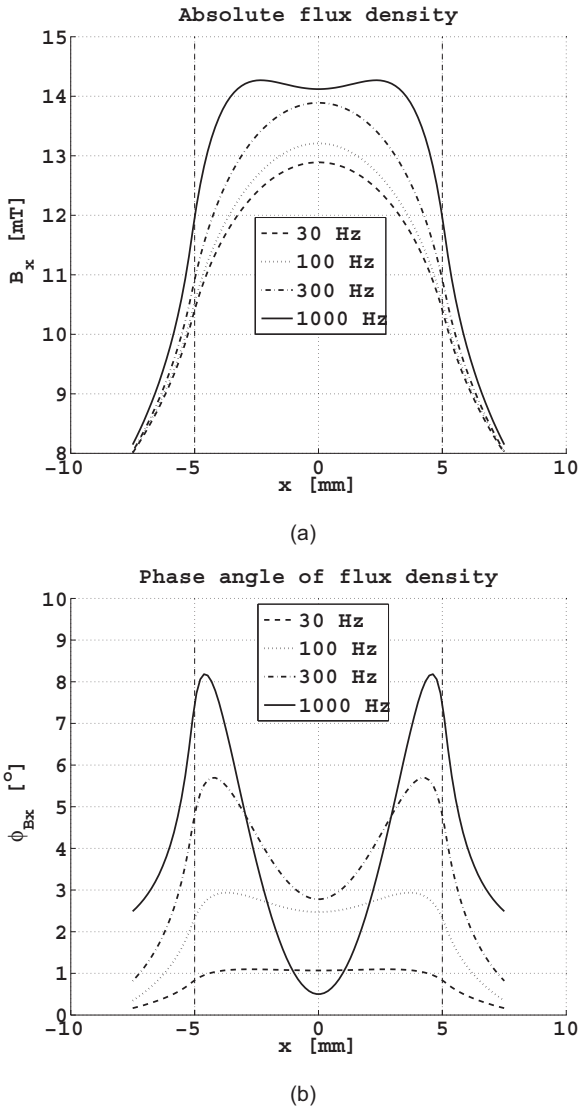

Fig. 8. Amplitude and phase angle of the x-component of flux density in direction parallel to the X axis.

Discussion

A simple formula for 2D skin effect in rectangular conductor was derived using simple boundary conditions of constant electric field strength. This decision was made in analogy to the wire of circular cross-section. In this case the constant value follows from symmetry considerations. For rectangular cross section of conductor the geometrical symmetry requires only the electric field strength symmetry on the surface. Other reason is the equipotential surfaces. In the DC case and for very low frequencies they are normal to the conductor axis. In the AC case we can expect that this condition is valid on the conductor surface. Of course, the effect of induced (eddy) currents can take a place on the surface too. As the only verification, the experimental measurement of the potential distribution on the conductor surface is necessary. In every case the analytical solution (11) can be considered as an approximating one.

Although the formula for the 1D layer is in textbooks [2], we have not found the formula (11) for the 2D case either in specialized monographs. This can be explained by the difficulty in the formulation of boundary conditions. The same is valid for the formula (16) for the magnetic field of thin straight conductor.

The main problem in the derived formula (11) is that it

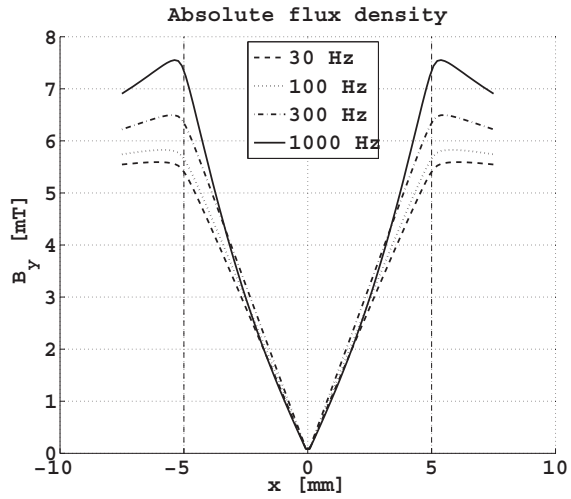

(a)

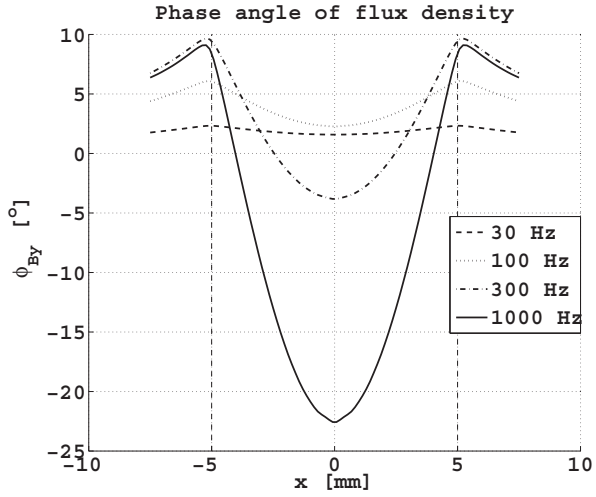

(b)

Fig. 9. Amplitude and phase of the y-component of flux density on line parallel to the X axis.

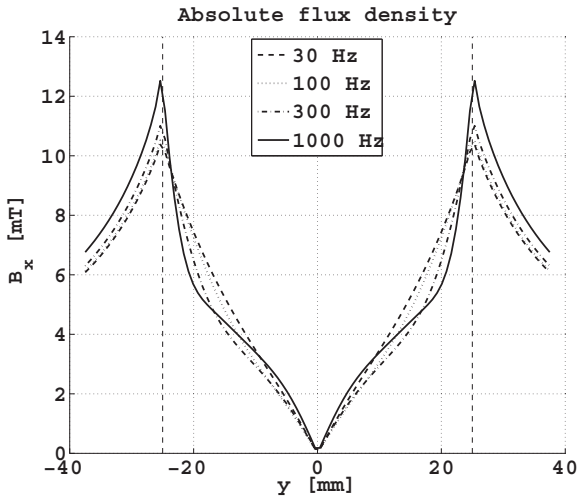

(a)

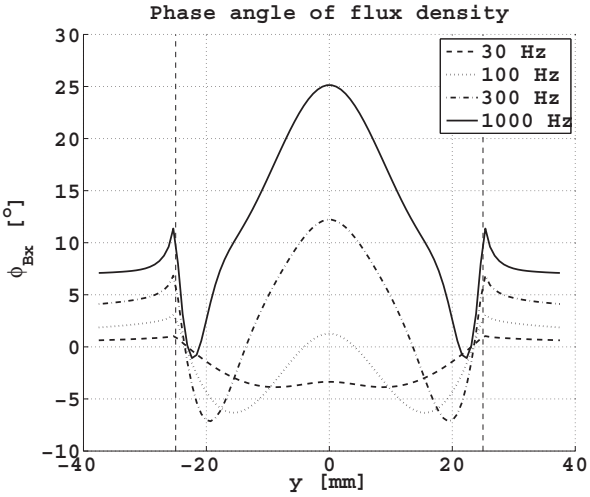

(b)

Fig. 10. Amplitude and phase of the x-component of flux density in direction parallel to the Y axis.

contains a product of complex functions; one component is a complex hyperbolic function of coordinate x and the other is the same function of coordinate y. The formula (11) is therefore nonlinear. The circuit theory states that all the relations must be linear. Then there is no difference in the use of real or imaginary component calculated from the formula. Each of them has the same physical meaning. Formulae for 1D layer skin effect are linear and there is no difference between the applications of real or imaginary component. The other can be obtained by a phase shift of +90° or -90°.

This statement is not valid for 2D skin effect. Real and imaginary component are quite different, which follows from Fig. 5 and Fig. 6 and was confirmed by the time simulation. Therefore, a question appears: what is their physical meaning and which of them can be used for further calculations, if any. In connection with this fact the pair amplitude and phase shift appears to be better defined. It means that careful, precise and well prepared experiment is necessary in order answer this basic question.

The simplest way is to measure the magnetic field produced by the current. It is a reason why extended calculations, respecting different conditions, were made. Only a small part of them is presented here.

We preferred numeric integration (NI) against very popular finite element (FEM) method. NI has several advantages. The user has a perfect control at every step of calculation, it uses simple formulae, there are no boundary conditions, the result can be obtained by predicted accuracy and the calculations is made at selected (and important) points only. Also the results are in the form applicable in typical graphical presentations.

The only advantage of FEM is its high speed, but by the use of parallel computation the calculation time can be reduced significantly. The parallel computation is realized in MATLAB by very simple commands. From the technical point of view, four core processors are, at least, in each new computer.

The calculated results reveal that the effect of skin effect on the flux density is measurable both in amplitude and phase. The use of phase measurement should be preferred, since the phase change is relatively high. On the other hand the realization of phase measurement is complicated. Since the phase shift is defined for the same frequency, we must measure the shift between total exciting currents and the exited component of flux density. There is no possibility to measure (or calculate from time function) the phase shift between different frequencies, as it is proposed from presented graphs.

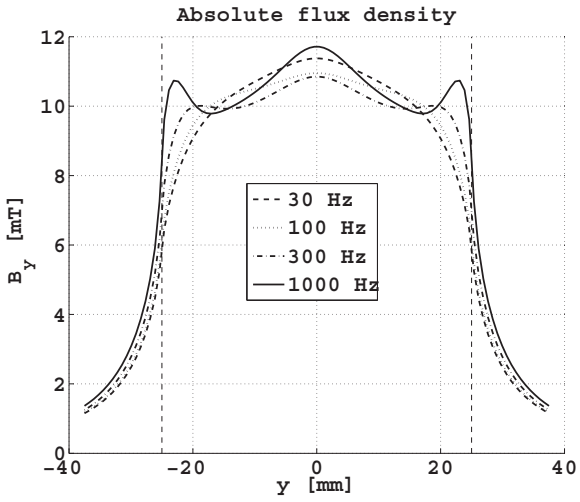

(a)

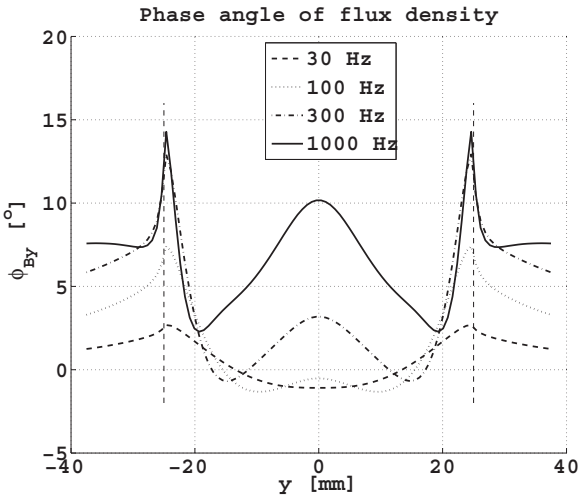

(b)

Fig. 11. Amplitude and phase of the y-component of flux density in direction parallel to the Y axis.

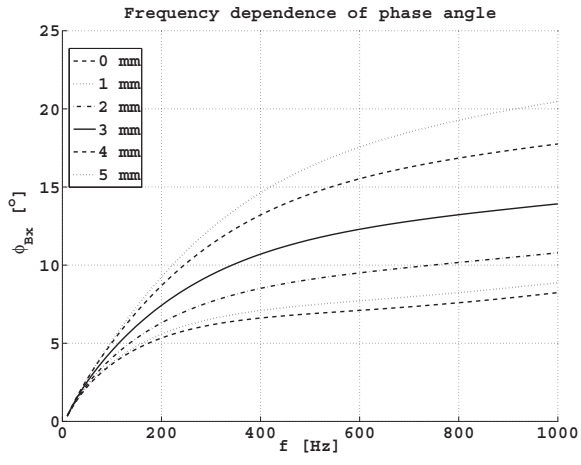

Fig. 12. Frequency dependence of phase shift on horizontal line.

The error of phase shift is seldom less than 1°. It means that the calculated phase shift of 10° can be measured by the accuracy of about 10 percent. This accuracy in selected cases can confirm or disapprove the theoretical results. As for amplitude, the accuracy is approximately similar. Both measurements of amplitude and phase shift are possible in

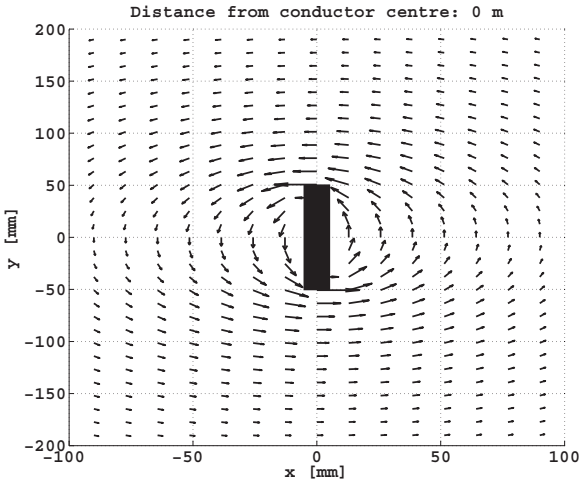

Fig. 13. Magnetic field in the central part of conductor.

our department, if the apparatus for conductor driving will be improved.

Two basic types of measurement are possible, at given point for varying frequency or for selected frequency at varying positions. The effect of current in reverse direction, see Fig. 5 and Fig. 7, has a low effect on amplitude that is non-measurable. By the use of precise phase measurement, the difference between calculations for real and absolute value of current density can be probably experimentally verified.

Conclusion

We have shown that skin effect has measurable effect on the magnetic field of the massive conductor. Only these measurements can verify all the main features of calculated current distribution.

At present time the department has an successfully tested apparatus for automated measurement of all the components of magnetic flux density with high accuracy in a plane [1]. For mechanically repeated measurement its accuracy is better than 1 percent. Therefore, most of the details in graphs for flux density component can be measured and the calculations and their interpretation can be verified. The application of phase measurement then will follow.

REFERENCES

[1] Mikolanda, T., Kosek, M., Richter, A.: Modeling and Measurement of Permanent Magnets, Acta Technica, (Institute of Thermomechanics AS CR), Vol. 55, No. 1, pp. 63-81, 2010. ISSN 0001-7043

[2] Sedlak, B., Stoll, I: Elektrina a magnetismus, 1. edition, Academia and Karolinum, 1993. ISBN 80-200-0172-7 (in Czech).

[3] Kosek, M. Truhlar. M. Richter, A: Detailed and Full Description of Skin Effect, Slaboproudy obzor, Vol. 64, pp. 9-12, 2008 (in Czech).

Acknowledgements

This work was supported by the student grant SGS 2010/7821 - Interactive mechatronic systems in technical cybernetics and the fund of Czech Science Foundation No. GACR 102/08/H081.

Authors: Prof. RNDr. Ing. Miloslav Kosek, email: miloslav.kosek@tul.cz CSc., Ing. Martin Truhlar, email: martin.truhlar@tul.cz, Prof. Ing. Ales Richter, CSc, email: ales.richter@tul.cz, Institute of Mechatronics and Computer Engineering, Faculty of Mechatronics, Informatics and Interdisciplinary Studies, Technical University of Liberec, Studentska 2, 461 17 Liberec 1 , Czech Republic